

Coexistence of Magnetization Relaxation and Dielectric Relaxation in a Single-Chain Magnet

Yue-Ling Bai,[†] Jun Tao,^{*,†} Wolfgang Wernsdorfer,[‡] Osamu Sato,^{*,§} Rong-Bin Huang,[†] and Lan-Sun Zheng[†]

Department of Chemistry, State Key Laboratory for Physical Chemistry of Solid Surfaces, Xiamen University, Xiamen 361005, P. R. China, Laboratoire Louis Néel-CNRS, 38042 Grenoble, Cedex 9, France, and Institute for Materials Chemistry and Engineering, Kyushu University, Kasuga, 816-8580, Fukuoka, Japan

Received September 15, 2006; E-mail: taojun@xmu.edu.cn; sato@cm.kyushu-u.ac.jp

Single-chain magnets (SCMs) featuring slow relaxation and large hysteresis of magnetization at low temperature have recently been attracting considerable attention owing to their potential for information storage applications at the molecular level. On one hand, the syntheses of SCMs is a great challenge in the field of molecule-based magnetism, because it is difficult to achieve experimentally the various properties that are essential ingredients of a perfect 1D Ising-type chain.¹ To date, several kinds of SCMs have been realized by the assembly of spin-carriers bridged by nitronyl nitroxides,² azides,³ Prussian blue anions and derivatives,⁴ and metal pyridine-2-aldoximate complexes.⁵ On the other hand, it is an appealing prospect to be able to create SCMs involving other physical properties that would make the SCMs into multifunctional materials. From this point of view, if SCMs could be crystallized into acentric or noncentric structures, it would be possible to obtain SCMs that possess nonlinear optical, ferroelectric or dielectric properties, and indeed, a family of SCMs that behave as NLO-active materials has recently been reported.⁶ However, no SCMs that exhibit dielectric properties have ever been reported. We recently reported intrachain ferromagnetic complexes that were built from planar Mn^{III}₃O units,⁷ and this has prompted us to investigate the possibility of finely tuning these structures to achieve SCMs. Here, we report on a novel SCM, [Mn^{III}₃O(Meppz)₃(EtOH)₄(OAc)] (**1**, Meppz = 3-(5-methyl-2-phenolate)pyrazolate), which was synthesized from a predesigned secondary building block [Mn^{III}₃O(Meppz)₃(EtOH)₅Cl] (**2**) and which demonstrated the coexistence of magnetization relaxation and dielectric relaxation properties.

1 was obtained from the metathesis reaction of **2** and sodium acetate in ethanol–acetonitrile solution (Supporting Information). X-ray structural analysis⁸ reveals that **1** is a chain complex in which stepwise ranked triangular Mn^{III}₃(μ₃-O²⁻) units are connected via anti–anti acetate groups (Figure 1). All of the manganese ions in the unit are octahedrally coordinated, with their Jahn–Teller elongation axes running in the direction of the chain. The manganese oxidation states have been established by bond–valence sum (BVS) calculations,⁹ charge balance considerations, and the observed Mn^{III} Jahn–Teller distortion. Each edge of the triangular unit is bridged by an η¹/η¹/μ-pyrazole group, and each vertex is coordinated terminally by an η¹-phenolate group, thus forming a nearly planar {Mn₃O(N₂O)₃} moiety with the central μ₃-O²⁻ ion located 0.0015 Å above the {Mn₃} plane. The hydrogen bonds between the ethanol molecules and the acetate groups play important roles in stabilizing the chain structure of **1** (Figure S1). It should be noted that the large steric hindrance of the ethanol molecules in

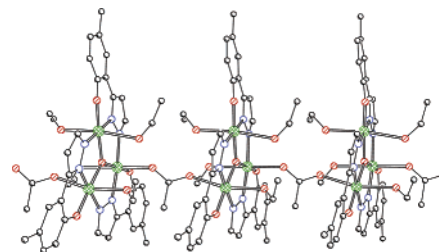


Figure 1. Chain structure of **1** viewed along the *c*-axis; the hydrogen atoms are omitted for clarity. Color codes: green, manganese; red, oxygen; blue, nitrogen; gray, carbon.

1 exerts a subtle influence on the relative interunit positions, and thus prevents the units from ranking in the same way as they do in the methanol analogue,⁷ causing **1** to crystallize in the *Cc* space group with a larger interchain shortest Mn···Mn separation (8.570 Å, Figure S2).

The DC magnetic susceptibility of **1** was measured in a field of 2.0 kOe in the temperature range from 2 to 300 K. The value of $\chi_M T$ is 7.95 cm³ K mol⁻¹ per Mn^{III}₃ unit at 300 K (Figure S4). This decreases in the high-temperature range and falls rapidly when $T < 100$ K upon cooling, reaching a minimum at 14 K. This behavior is indicative of dominant intracluster antiferromagnetic interactions. Below T_{\min} , $\chi_M T$ increases to a maximum of 3.2 cm³ K mol⁻¹ at 7 K and then falls, which may arise from zero-field splitting, Zeeman effects, and/or weak interchain interactions. These data were fitted to the theoretical expression for an isosceles triangle (J_1, J_2) model above 25 K by treating the intrachain interunit interactions with mean-field approximations (zJ), to give $J_1 = -1.87$ cm⁻¹, $J_2 = -5.61$ cm⁻¹, $g = 1.99$ and $zJ = -0.014$ cm⁻¹. The negative zJ value indicates weak antiferromagnetic interactions via acetate bridges, which is different from the methanol analogue in which ferromagnetic interactions obviously exist.⁷ The upsurge at 7 K may therefore be due to spin-canting interactions. It is well-known that the planar Mn^{III}₃O unit is expected to experience magnetic frustration at low temperature; its S value for the ground state varies from 0, 1 to 2 based on the calculated J_1/J_2 values.¹⁰ The J_1/J_2 value (0.33) of **1** indicates an $S = 1$ ground state according to theoretical prediction. Extrapolation the $\chi_M T \sim T$ plot further confirms an $S = 1$ rather than $S = 2$ ground state (Figure S5), which is co-incident with that of **2** (Figure S6).

AC susceptibility measurements were performed in the range 2–6 K in a 3 G AC field oscillating at 1–1500 Hz. Below 4 K, the strong frequency-dependent decrease in the in-phase signal (χ_M') with the appearance of the out-of-phase signal (χ_M'') is directly associated with the slow magnetization relaxation of the SCMs (Figure 2 and Figure S7). The SCM behavior of **1** was confirmed by measuring a single-crystal hysteresis loop and associated

[†] Xiamen University.

[‡] Laboratoire Louis Néel-CNRS.

[§] Kyushu University.

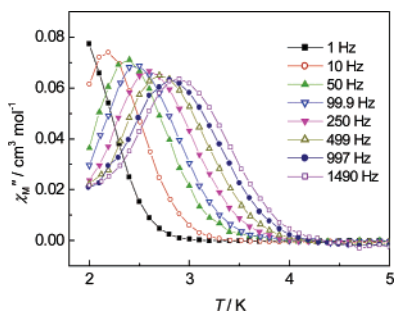


Figure 2. The out-of-phase (χ'') AC susceptibility signal of **1**.

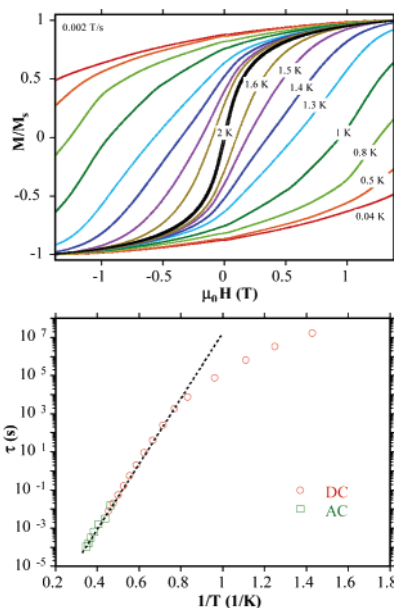


Figure 3. (Top) M vs H hysteresis loop for a single crystal of **1**. M is normalized to its saturation value. (Bottom) Arrhenius plot using AC and DC data. The dashed line is the fit of the thermally activated region to the Arrhenius equation.

relaxation using a micro-SQUID.¹¹ Hysteresis (Figure 3, top) was observed below 2.0 K, with coercivity increasing with decreasing temperature and increasing field sweep rate, as expected for an SCM. Figure 3 (bottom) depicts the τ versus $1/T$ plot from a combination of single-crystal DC relaxation decay measurements and AC measurements based on the Arrhenius relationship $\tau = \tau_0 \exp(U_{\text{eff}}/k_B T)$, where U_{eff} is the effective relaxation barrier, τ is the relaxation time, and k_B is the Boltzmann constant. The slope of the thermally activated region gave $U_{\text{eff}} = 39.9$ K and $\tau_0 = 1.2 \times 10^{-10}$ s. The low-temperature deviations from the straight line may be due to finite-size effects.

Considering that **1** crystallizes in the noncentric space group Cc and exhibits a highly anisotropic 1D structure, it may belong to that class of dipole chains whose dielectric relaxation in the time domain and the frequency domain can also be studied by using Glauber dynamics based on the kinetic Ising model. Figure 4 shows the dielectric imaginary part of **1**, where the peak temperature of the imaginary part shifts to the higher temperature side with increasing frequency, which clearly indicates a relaxation process. Though **1** is nonferroelectric, the relaxation time also follows the Vogel–Fulcher relationship¹² $\tau = \tau_0 \exp[E/k_B(T - T_{\text{VF}})]$ as in many relaxor ferroelectrics, where $\tau = 1/2\pi f$, when f is the frequency at which the dielectric loss shows a maximum at temperature T , k_B is the Boltzmann constant, T_{VF} is the Vogel–Fulcher temperature and is considered to be the temperature below which the relaxing dipoles freeze and become static. From Figure 4, the activity energy E and

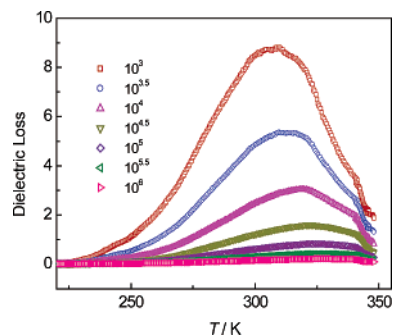


Figure 4. Temperature dependence of dielectric loss of **1** at different frequencies.

the relaxation time τ_0 are estimated as being approximately 0.21 eV and 3.1×10^{-17} s, respectively. This behavior may be assigned to the polar structure and/or a chain microvibration that results in an overall chain–chain dipolar relaxation process.^{12c,d}

In conclusion, we have synthesized a new SCM (**1**) that was prepared via a step-by-step method from a predesigned building block (**2**) with an $S = 1$ ground state. The most important aspect of this is that **1** is the first example of a compound that exhibits the coexistence of magnetization relaxation and dielectric relaxation in a SCM.

Acknowledgment. This work was supported by the National Natural Science Foundation of China (Grant 20301014).

Supporting Information Available: Synthetic details, ORTEP drawing of **1**, additional figures, and X-ray data for **1** and **2** in CIF format. This material is available free of charge via the Internet at <http://pubs.acs.org>.

References

- (1) Glauber, R. J. *J. Math. Phys.* **1963**, *4*, 294.
- (2) (a) Caneschi, A.; Gatteschi, D.; Lalioti, N.; Sangregorio, C.; Sessoli, R.; Venturi, G.; Vindigni, A.; Rettori, A.; Pini, M. G.; Novak, M. A. *Angew. Chem., Int. Ed.* **2001**, *40*, 1760. (b) Bogani, L.; Sangregorio, C.; Sessoli, R.; Gatteschi, D. *Angew. Chem., Int. Ed.* **2005**, *44*, 5817. (c) Bernot, K.; Bogani, L.; Caneschi, A.; Gatteschi, D.; Sessoli, R. *J. Am. Chem. Soc.* **2006**, *128*, 7947.
- (3) (a) Liu, T.-F.; Fu, D.; Gao, S.; Zhang, Y.-Z.; Sun, H.-L.; Su, G.; Liu, Y.-J. *J. Am. Chem. Soc.* **2003**, *125*, 13976. (b) Lecren, L.; Roubeau, O.; Coulon, C.; Li, Y.-G.; Le Goff, C. F.; Wernsdorfer, W.; Miyasaka, H.; Clérac, R. *J. Am. Chem. Soc.* **2005**, *127*, 17353.
- (4) (a) Ferbinteanu, M.; Miyasaka, H.; Wernsdorfer, W.; Nakata, K.; Sugiura, K.; Yamashita, M.; Coulon, C.; Clérac, R. *J. Am. Chem. Soc.* **2005**, *127*, 3090. (b) Lescouëzec, R.; Toma, L. M.; Vaissermann, J.; Verdager, M.; Delgado, F. S.; Ruiz-Pérez, C.; Lloret, F.; Julve, M. *Coord. Chem. Rev.* **2005**, *249*, 2691 and references therein. (c) Toma, L. M.; Lescouëzec, R.; Pasán, J.; Ruiz-Pérez, C.; Vaissermann, J.; Cano, J.; Carrasco, R.; Wernsdorfer, W.; Lloret, F.; Julve, M. *J. Am. Chem. Soc.* **2006**, *128*, 4842.
- (5) (a) Clérac, R.; Miyasaka, H.; Yamashita, M.; Coulon, C. *J. Am. Chem. Soc.* **2002**, *124*, 12837. (b) Miyasaka, H.; Clérac, R. *Bull. Chem. Soc. Jpn.* **2005**, *78*, 1725 and references therein.
- (6) Bogani, L.; Cavigli, L.; Bernot, K.; Sessoli, R.; Gurioli, M.; Gatteschi, D. *J. Mater. Chem.* **2006**, *16*, 2587.
- (7) Tao, J.; Zhang, Y.-Z.; Bai, Y.-L.; Sato, O. *Inorg. Chem.* **2006**, *45*, 4877.
- (8) Crystal data for **1**: $C_{40}H_{51}Mn_3N_5O_{10}$, $M = 940.69$, monoclinic, space group Cc (No. 9), $T = 173(2)$ K, $a = 21.708(4)$, $b = 25.104(5)$, $c = 7.726(2)$ Å, $\beta = 98.32(3)^\circ$, $V = 4166.0(14)$ Å³, $Z = 4$, $D_c = 1.500$ g/cm³, $R_1 = 0.0386$, $wR_2 = 0.0838$. Crystal data for **2**: Supporting Information.
- (9) (a) Liu, W.; Thorp, H. H. *Inorg. Chem.* **1993**, *32*, 4102. (b) BVS for Mn1, Mn2, and Mn3 are 3.12, 3.19, and 3.18, respectively. BVS for O²⁻ ion is 1.86.
- (10) Jones, L. F.; Rajaraman, G.; Brockman, J.; Murugesu, M.; Sanudo, E. C.; Raftery, J.; Teat, S. J.; Wernsdorfer, W.; Christou, G.; Brechin, E. K.; Collison, D. *Chem.–Eur. J.* **2004**, *10*, 5180.
- (11) Wernsdorfer, W. *Adv. Chem. Phys.* **2001**, *118*, 99.
- (12) (a) Tagantsev, A. K. *Phys. Rev. Lett.* **1994**, *72*, 1100. (b) Ranjan, R.; Dviwedi, A. *Solid State Commun.* **2005**, *136*, 394. (c) Tang, Y.-Z.; Huang, X.-F.; Song, Y.-M.; Chan, P. W. H.; Xiong, R.-G. *Inorg. Chem.* **2006**, *45*, 4868. (d) Ye, Q.; Song, Y.-M.; Wang, G.-X.; Chen, K.; Fu, D.-W.; Chan, P. W. H.; Zhu, J.-S.; Huang, S.-D.; Xiong, R.-G. *J. Am. Chem. Soc.* **2006**, *128*, 6554.

JA066679+